Paper No.

9098

Verification of an Electrochemical Model for Aqueous Corrosion of Mild Steel for H_2S Partial Pressures up to 0.1 MPa

Saba Navabzadeh Esmaeely, Bruce Brown, Srdjan Nesic

Institute for Corrosion and Multiphase Technology,

Department of Chemical and Biomolecular Engineering, Ohio University,

342 W. State Street, Athens, Ohio, 45701.

ABSTRACT

Hydrogen sulfide (H_2S) corrosion of mild steel is a serious concern in the oil and gas industry. However, H_2S corrosion mechanisms, specifically at high partial pressures of H_2S (pH_2S), have not been extensively studied because of experimental difficulties and associated safety issues. The current study was conducted under well-controlled conditions at pH_2S of 0.05 and 0.096 MPa. The pH range used was from pH 3.0 to pH 5.0, at temperatures of 30 and 80˚C, and with rotating cylinder speeds of 100 rpm and 1000 rpm. Short-term exposures, lasting between 1.0 and 1.5 hours, were used to avoid formation of any protective iron sulfide layers. The experimental results were compared with a recent mechanistic model of sour corrosion developed by Zheng, *et al.* (2014). This model was based on corrosion experiments conducted at low pH_2S (0.0001 – 10 kPa) and is applicable only to conditions where protective iron sulfide layers do not form. The validity of the model at higher pH_2S was examined, as it was uncertain if the mechanisms identified at lower pH_2S were still valid. The comparison with the experimental results obtained in the present study indicated a good agreement between the model and the measurements. This confirmed that the physico-chemical processes underlying H_2S corrosion in the absence of protective iron sulfides are very similar across a wide range of H_2S aqueous concentrations. It also demonstrated that the mechanistic corrosion model was reasonable when extrapolating from low to high pH_2S.

Key words: corrosion rate, H_2S, modeling

INTRODUCTION

The role of hydrogen sulfide (H_2S) on aqueous mild steel corrosion has been one of the concerns of corrosion researchers since 1940 [1–13]. Ewing[14] and Sardisco, et al., [15] were among the first scholars to initiate controlled H_2S corrosion experimentation which was later continued by other researchers [13,16–20]. The focus of much of the H_2S related studies in the past was on iron sulfide formation and the resulting effect on corrosion[3,21–23]. The vast majority of the available research results come from experiments conducted at lower H_2S partial pressures ($pH_2S < 10^{-2}$ MPa). Over the past few decades, a significant number of new oil and gas fields are sour, ranging from a few ppm up to 15-20 mol% H_2S (e.g., the Kashagan Field[24]). This indicated a growing need for better understanding of H_2S corrosion mechanisms and more effective prediction tools, particularly at higher pH_2S.

Uncertainties related to modelling of H_2S corrosion are particularly pronounced at higher pH_2S. Under those conditions, limited results are available. Therefore, most of the models developed so far are based on lower pH_2S. Despite the progress in understandings of H_2S corrosion [1-35], there is still a lack of systematic studies where the parameter space has been explored in an organized way. Again, the problem is even more pronounced at higher pH_2S where the challenges associated with conducting experiments are much bigger. Corrosion data that have been reported under these conditions in the open literature are very few, with widely scattered operating conditions.

There has been substantial progress in understanding and modeling of H_2S-related corrosion since the late 90s. In 2009, Sun, *et al.*,[19] proposed a mechanistic H_2S model that accounted for iron sulfide layer formation. It assumed that the corrosion rate was always under mass transfer control with the iron sulfide layer being dominant, and it did not take into account the kinetics of electrochemical reactions. While this has been proven to be an overly restrictive assumption, the work conducted by Sun, *et al.,*[19] provided a foundation for further investigation and modeling of H_2S corrosion mechanisms in a more systematic way.

In 2014 and 2015, Zheng, *et al.*, [20,25] developed a mechanistic model of pure H_2S and mixed CO_2/H_2S corrosion of mild steel that considered both the electrochemical and mass transfer controlled reactions. This model calculates the corrosion rate in the absence of iron sulfide layers. The authors were able to demonstrate that when mild steel was exposed to aqueous H_2S, the direct reduction of H_2S occurs on the steel surface as an additional hydrogen evolution reaction. The model was validated with experimental data from corrosion experiments conducted in an aqueous solution sparged with H_2S at partial pressures from 10^{-7} to 10^{-2} MPa. [20,25]

The focus of the current study is on the higher pH_2S and the corrosion mechanisms of mild steel at those conditions. One of the key hypotheses is that the mechanistic model [20,25] based on low pH_2S data, will perform at higher pH_2S. To prove this, one needs reliable experimental data at higher pH_2S, thus a number of experimental studies were found in the available open literature. The choice of literature data was made according the following criteria: the corrosion study had to be comprehensively reported, including a proper description of the experimental set-up, procedures and data analysis. For example studies that failed to describe the water chemistry or some other key experimental parameters were not considered, even if the corrosion results were reported. Furthermore, only the experimental data that were obtained in short exposures, prior to formation of protective iron sulfide corrosion product layers were considered, in order to compare with the model [20,25].

The results of this exercise is given in Figure 1(a), which shows parity plots where all of the selected experimental corrosion rate data from the open literature at high pH_2S are plotted vs. the predictions made by the model. The solid lines in Figure 1 represent a perfect agreement, while the dashed lines represent a factor of two difference between the measured and predicted values. The different colors of the symbols indicate data from different experimental conditions and/or different studies.

In this comparison, it appears that the model over-predicts the majority of the measured corrosion rates. However, before drawing any conclusions about the performance of the model, it is essential to reconfirm that the experimental data were consistent and suitable for the present exercise. All the outliers, shown on the parity plot in Figure 1(a), were generated in a single experimental study by Omar, *et al*.[24]. The authors presented time series from long term experiments, hence only the data points reported at time "zero" were used here. After analyzing the data of Omar, *et al*.[24] it seems likely that an iron sulfide layer had formed on the specimens' surface prior to that first reported corrosion rate measurement. The challenge the authors faced was in the fast kinetics of iron sulfide formation reactions in high H_2S containing environments[26]. They reported lower corrosion rates for higher pH_2S and pCO_2 (as listed in TABLE 1) which can only happen if protective iron carbonate and/or iron sulfide layers formed. Consequently, these data points were eliminated from the present study.

The reduced number of data points collected at high pH_2S now appears to be within a factor of two of the model predictions, as shown in Figure 1(b). The remaining eight data points came from three different high pH_2S corrosion studies, with widely different conditions and with no additional information on underlying corrosion mechanisms. This illustrates that there is a clear lack of reliable, systematically collected, coherent corrosion data from high pH_2S experiments, based on sound electrochemical measurements. Therefore, the present study is meant to fill this gap, and provide a solid base for verification of mechanisms and models for mild steel corrosion in high pH_2S environments.

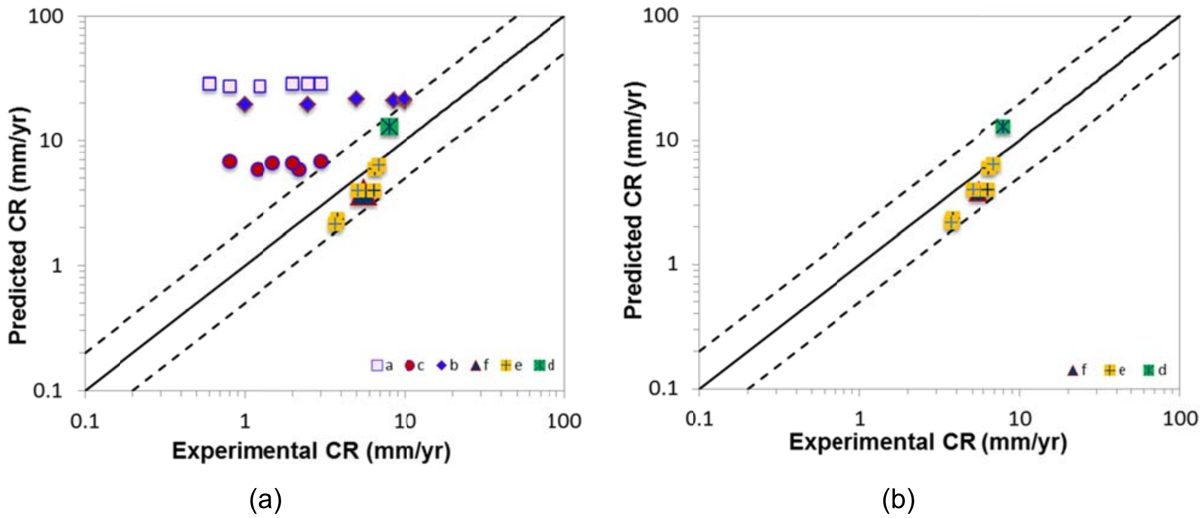

Figure 1. Parity plot of the predicted data using Zheng's model when there is no iron sulfide layer *vs*. experimental data at higher pH_2S. [24,27–29]

TABLE 1

Summary of Results

Test Conditions	Reported Corrosion Rate mm/y	Predicted Corrosion Rate mm/y	Reference	Legend
1 MPa H_2S; 0.33 MPa CO_2; pH 3.1; 1, 3 and 5 m/s; 80˚C	1 to 10	19 to 21	Omar *et al.*, [24]	b
1 MPa H_2S; 0.33 MPa CO_2; pH 3.2; 1, 3 and 5 m/s; 25˚C	2 to 3	5 to 6	Omar *et al.*,[24]	c
3 MPa H_2S; 1 MPa CO_2; pH 3.0; 1, 3 and 5 m/s; 80˚C	0.8 to 2	27 to 28	Omar *et al.*, [24]	a
0.14 MPa H_2S; 0.06 MPa CO_2; pH 4.5; 1 m/s; 60˚C	5.5	3.8	Kvarekval *et al.*, [27]	d
0.088 MPa H_2S; pH 4.2; 50˚C	3.7	2.4	Abayarathna *et al.*, [28]	e
0.069 MPa H_2S; pH 4.2; 70˚C	5.1	3.9	Abayarathna *et al.*, [28]	e
0.03 MPa H_2S; pH 4.2; 90˚C	6.9	6.3	Abayarathna *et al.*, [28]	e
0.044 MPa H_2S; 0.044 MPa CO_2; pH 4.2; 50˚C	3.8	2.3	Abayarathna *et al.*, [28]	e
0.034 MPa H_2S; 0.034 MPa CO_2; pH 4.2; 70˚C	6.4	3.6	Abayarathna *et al.*, [28]	e
0.015 MPa H_2S; 0.015 MPa CO_2; pH 4.2; 90˚C	6.5	5.8	Abayarathna *et al.*, [28]	e
1.6 MPa H_2S; 90˚C	8	12.8	Liu *et al.*, [29]	f

EXPERIMENTAL METHOD AND SET-UP

Experiments were conducted in a glass cell (see Figure 2), which was filled with 2 liters of deionized water and 60.6 g NaCl to obtain a 3.0 wt% solution. The solution was deoxygenated by purging with N_2 for 3 hours and was then saturated with H_2S by continuously purging the solution with H_2S gas throughout the remainder of the experiment. The gas outlet was scrubbed using a 5 M solution of sodium hydroxide (NaOH) and a series of dry carbon scrubbers. The solution pH was adjusted to the desired value by addition of a deoxygenated hydrochloric acid (HCl) or a NaOH solution. It was deemed that equilibrium in the solution was reached after approximately 1 hour after the introduction of H_2S gas into the glass cell.

A cylindrical API[1] 5L X65 steel specimen was sequentially polished with 150, 400, and 600 grit sand paper, rinsed with isopropyl alcohol in an ultrasonic bath, and air dried. It was then mounted onto the RCE rotator and inserted into the glass cell for electrochemical measurements. The rotator was set to the desired rotational speed and the corrosion measurements were initiated.

Electrochemical measurements were conducted using a three electrode setup with a mild steel rotating cylinder (RCE) as the working electrode (WE). A platinum mesh plate was used as the counter electrode (CE). An external saturated silver/silver chloride (Ag/AgCl) reference electrode (RE) was connected using a KCl salt bridge *via* a Luggin capillary. Open circuit potential (OCP), measurements were done first to ensure that a reasonably stable state was reached, where the OCP drift was less than 1 mV per min and the magnitude of the OCP fluctuation was less than 1 mV (this occurred typically within the first 5 min). The OCP measurements were immediately followed by electrochemical impedance spectroscopy (EIS), in order to determine the solution resistance (IR drop). Then, the linear polarization resistance (LPR) measurements were conducted in order to estimate the polarization resistance (R_P) and the corrosion rate. Finally, potentiodynamic measurements were conducted by first sweeping the potential from the OCP in the cathodic direction. After the OCP stabilized (usually within 10 min) the anodic potential sweep was performed.

During the LPR measurements, the WE was polarized ±5 mV from the OCP in order to determine the (R_P), using a scan rate of 0.125 mV/s. The measured R_P was corrected for the solution resistance that was obtained from the high frequency portion of the EIS spectrum (frequency range around 5 kHz). The linear polarization constant, B = 23 mV/decade, was used in the current work based on comparison of LPR measurements with weight loss [20]. Potentiodynamic sweeps were conducted at a rate of 5 mV/s. While this is generally considered a very fast sweep rate, where transient effects could interfere, it was an imperative to complete the measurements in the shortest possible time, in order to avoid formation of protective iron sulfide layers. Also, the fast sweep rate minimized the atomic hydrogen diffusion in to the steel, which allowed the surface to recover to the OCP in a shorter period. In order to confirm that the fast sweep rate was acceptable, the potentiodynamic sweeps obtained at a low pH and low temperature (where formation of iron sulfide was slower) were compared by using sweep rates of 1 mV/s and 5 mV/s, with no substantial difference seen. Each potentiodynamic sweep was corrected for the ohmic drop due to solution resistance. The experiments were conducted at three different pH, two different velocities and temperatures as summarized in TABLE 2.

.

---

[1] American Petroleum Institute (API), 1220 I St. N.W. Washington, DC 20005-4070.

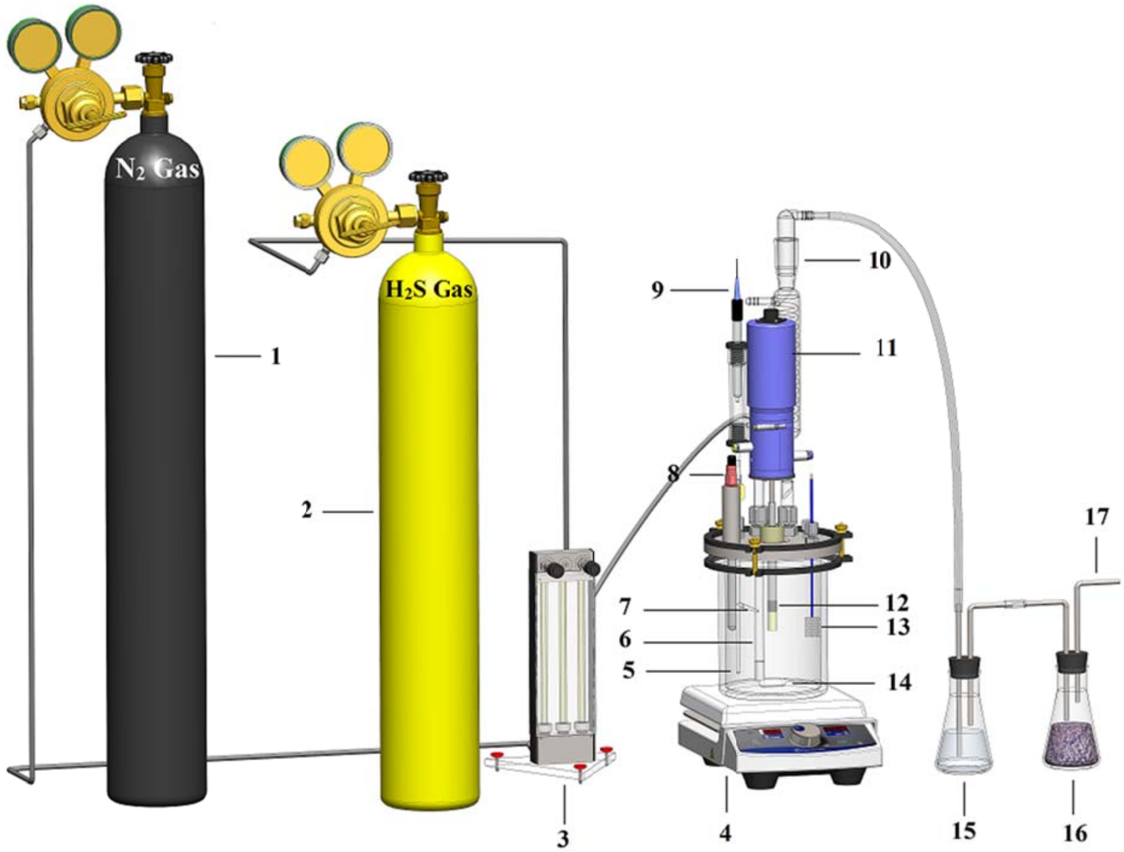

Figure 2. Experimental setup with 1. N_2 gas cylinder 2. H_2S gas cylinder 3. rotameter 4. hot plate 5. temperature probe 6. gas inlet 7. Luggin capillary 8. pH-electrode 9. reference electrode 10. condenser 11. rotating cylinder shaft 12. working electrode 13. platinum counter electrode 14. stir bar (½″ inch length) 15. sodium hydroxide solution 16. carbon scrubber 17. gas outlet[♣]

TABLE 2

Experiment Matrix

Parameters	Conditions
Total Pressure	0.1 MPa
Temperature	30 and 80°C
Solution	3 wt.% NaCl
Test Condition	1000, 100 rpm
Material	API 5L X65
Methods	LPR, EIS, and Potentiodynamic Sweep
pH_2S in the Gas Phase	0, 0.053 and 0.096 MPa
pH Value	2.0, 3.0, 4.0 and 5.0 (± 0.1)

♣ Image is courtesy of Cody Shafer

RESULTS AND DISCUSSION

To establish a baseline, the model calculations[20,30] were first compared to potentiodynamic sweep data obtained in N_2 saturated aqueous solutions at pH 2.0 and pH 3.0; the data were collected at room temperature in the absence of H_2S. The experimental repeatability and accuracy of the electrochemical measurements were quantified by repeating the experiments multiple times as shown in Figure 3. There, the points represent the average value of the current obtained in different repeats and the error bars denote the maximum and minimum values, all taken at the exactly the same potential.

Figure 3(a) shows that for pH 2.0, the experimentally measured current densities deviated from the model predictions by approximately 50% in the charge transfer region and about 25% in the limiting current region. The deviation seen in the limiting currents is statistically significant and possibly stems from excessive evolution of hydrogen gas bubbles, which altered the otherwise well controlled mass transfer conditions in the vicinity of the electrode surface[12] at high current densities. The apparently large discrepancy seen in the charge transfer region of the potentiodynamic sweeps is not as significant, since the difference between calculated values and the averages of the measured values is of the same order of magnitude as the variation within the measured values themselves. In addition, it should be pointed out that the model was not developed to accurately predict in such low pH conditions and there may be some physico-chemical processes that are not captured well for the case of steel corrosion in strong acids. However, this is not a big concern since pH 2.0 lays outside the typical pH range seen in most H_2S dominated conditions.

The situation is markedly better at pH 3.0 as shown in Figure 3(b), where a very good agreement between the model and the measured data is seen, particularly for the cathodic reaction. These two sets of results obtained in the absence of H_2S confirm that, both the model performance and the experimental procedures/techniques were at an acceptable level, providing a good foundation for the next step – comparison of the model with the data obtained in H_2S saturated conditions.

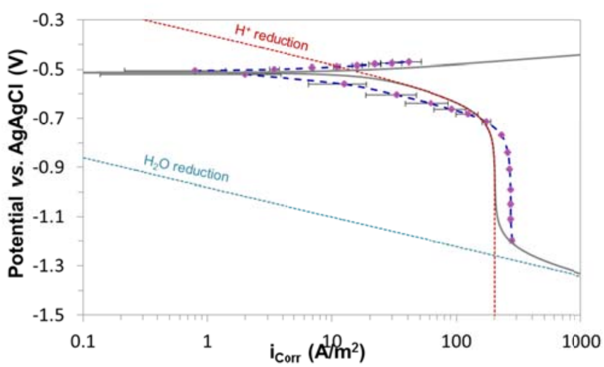

(a)

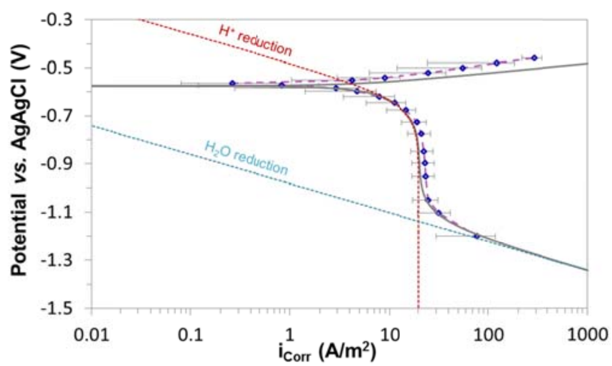

(b)

Figure 3. Potentiodynamic sweeps on mild steel in N_2 purged solutions, 1 wt. % NaCl, 30˚C, and 1000 rpm RCE, scan rate 5 mV/S, (a) pH 2.0 (2 repeats); (b) pH 3.0 (6 repeats).

If we now turn our focus to H_2S saturated solution, the effect of pH is shown in Figure 4. In Figure 4(a) the measured data points show an average obtained from five repeats, conducted at the pH 3.0. There is a very good agreement between the measured data and the calculated ones, particularly at the lower current densities (<10 A/m^2). The deviation in the limiting current at very high current densities (>500 A/m^2) was probably due to excessive formation of hydrogen gas bubbles at the electrode surface. The existence of the so called "double wave" comes from the two independent cathodic reactions and their limiting currents. [20,31.]

Similar results were obtained at pH 4.0, see Figure 4(b), which shows the averages of the data collected from four repeated experiments. Data from the experiments conducted at pH 5.0 are presented in Figure 4(c), which shows the averages from experiments repeated six times. It is clear that at the higher pH values, the reduction of H_2S dominates the rate of the cathodic reaction, as a result of a lower rate of H^+ reduction due to a lower concentration of H^+ ions. There seems to be a slight deviation between the measured and calculated Tafel slope for H_2S reduction, which is difficult to explain. It may be due to a measurements error obtained at the higher current densities (>10 A/m^2) or a result of the inaccuracy of the model at these conditions. Either way, this is not expected to affect the corrosion rate calculation in a significant way, since the corrosion current densities are typically below 10 A/m^2.

For data collected at pH 5.0, presented in Figure 4(c), there is an approximately 50 mV deviation between the calculated and the measured OCP. This problem is most likely associated with the modeling of the anodic (iron dissolution) current. To confirm this and eliminate any possible experimental error associated with iron sulfide layer formation during the cathodic sweeps (which were conducted first), a new experiment was organized where the anodic sweep was conducted on a freshly polished specimen. The results were consistent and provided conclusive evidence that the OCP deviation was not a result of erroneous measurements. It is difficult to postulate what the exact problem is, without a more extensive investigation of the anodic reaction in H_2S environments, which exceeds the scope of the present paper. It is worth noting that the effect of adsorbed OH^- on the rate of anodic iron dissolution was not considered in the model [20]. However, whether this is the main cause of the discrepancy seen at pH 5.0 requires further research.

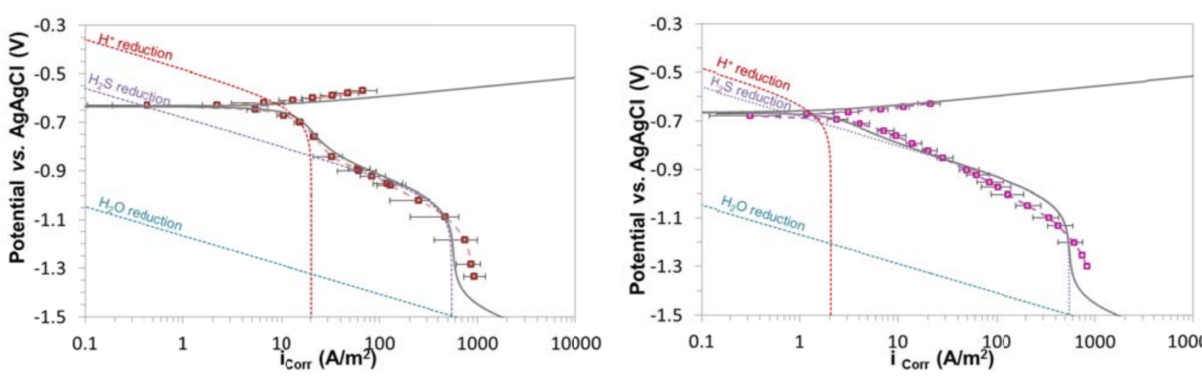

(a) (b)

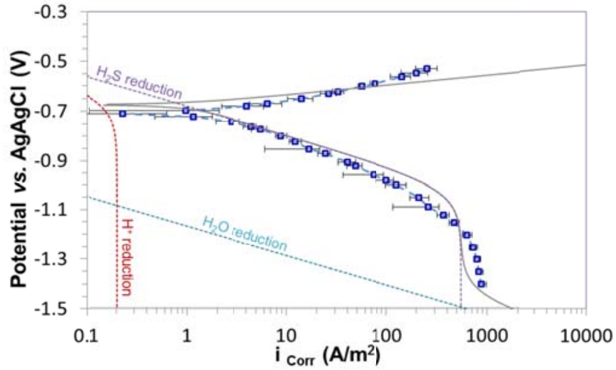

(c)

Figure 4. Potentiodynamic sweeps on mild steel in H_2S saturated solution with 0.096 MPa H_2S (960,000 ppm) in the gas phase, 3 wt. % NaCl, 30˚C, and 1000 rpm RCE, scan rate 5 mV/s, (a) pH 3.0 (5 repeats); (b) pH 4.0 (4 repeats); (c) pH 5.0 (6 repeats).

The performance of the model at lower velocity is shown in Figure 5. This 100 rpm experiment was repeated twice. In this condition the measured data are in good agreement with the calculated ones, particularly at the lower current densities. At the higher current densities the discrepancy seen in the cathodic limiting current is due to the abovementioned hydrogen gas bubble evolution. For the anodic reaction, the deviation is most likely due to accumulation of ferrous ions at the steel surface at lower rotation speed and formation of an iron sulfide layer, leading to some type of "pre-passivation" behavior.

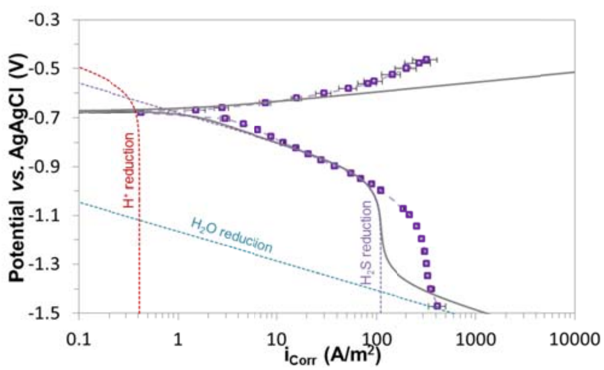

Figure 5. Potentiodynamic sweeps on mild steel in H_2S saturated solution with 0.096 MPa H_2S (960,000 ppm) in the gas phase, pH 4.0, 3 wt. % NaCl, 30˚C, and <u>100 rpm</u> RCE, scan rate 5 mV/s, 2 repeats.

Data from higher temperature are presented in Figure 6, where the average of data from two potentiodynamic sweeps conducted at 80˚C is shown. It is important to mention that the pH_2S in these experiments was 0.053 MPa due to an increase of the water vapor in the glass cell that was at atmospheric conditions. Similar to previous conditions, at lower current densities there is a very good agreement between measured and calculated data, while the discrepancies at higher current densities are present for the same reasons as described above.

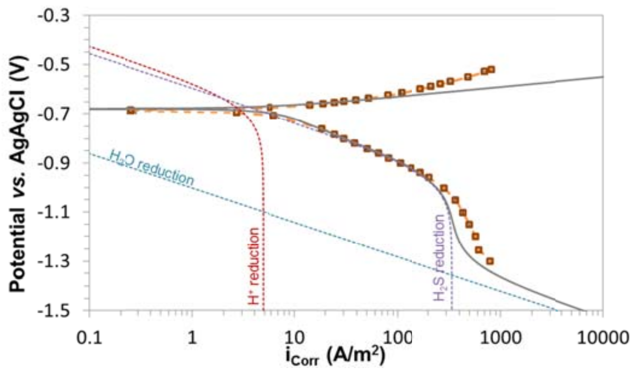

Figure 6. Potentiodynamic sweeps on carbon steel in H_2S saturated solution with 0.053 MPa H_2S (530,000 ppm) in the gas phase, pH 4.0, 3 wt. % NaCl, 80°C, and 1000 rpm RCE, scan rate 5 mV/S, 2 repeats.

LPR measurements were conducted in each experiment to measure the uniform corrosion rate, and the results are summarized in Figure 7. The bars are the average of the measured corrosion rate values from repeated experiments, and the error bars show the maximum and minimum deviation from the average. As would be expected, the bare steel corrosion rate decreased with pH, increased with velocity and temperature. The comparison of calculated and measured uniform corrosion rates is shown in Figure 8 as a parity plot. The open symbols are the original experimental data reported by Zheng, *et al.*,[20] for lower pH_2S, which are almost in perfect agreement with the predicted corrosion rate. This is to be expected as the model [20] was developed and calibrated using the same low pressure data (ranging from 10^{-7} – 10^{-2} MPa pH_2S). The bold squares in Figure 8 are the results from the current study, conducted at approximately 0.1 MPa pH_2S, and are also in good agreements with the model calculations. This is of importance as the current data were obtained in an independent study conducted at a much higher pH_2S.

The current study confirmed that the physico-chemical processes underlying H_2S corrosion in the absence of protective iron sulfides are very similar across a wide range of pH_2S. It also demonstrated that the abovementioned mechanistic corrosion model is valid across a broad range of pH_2S conditions.

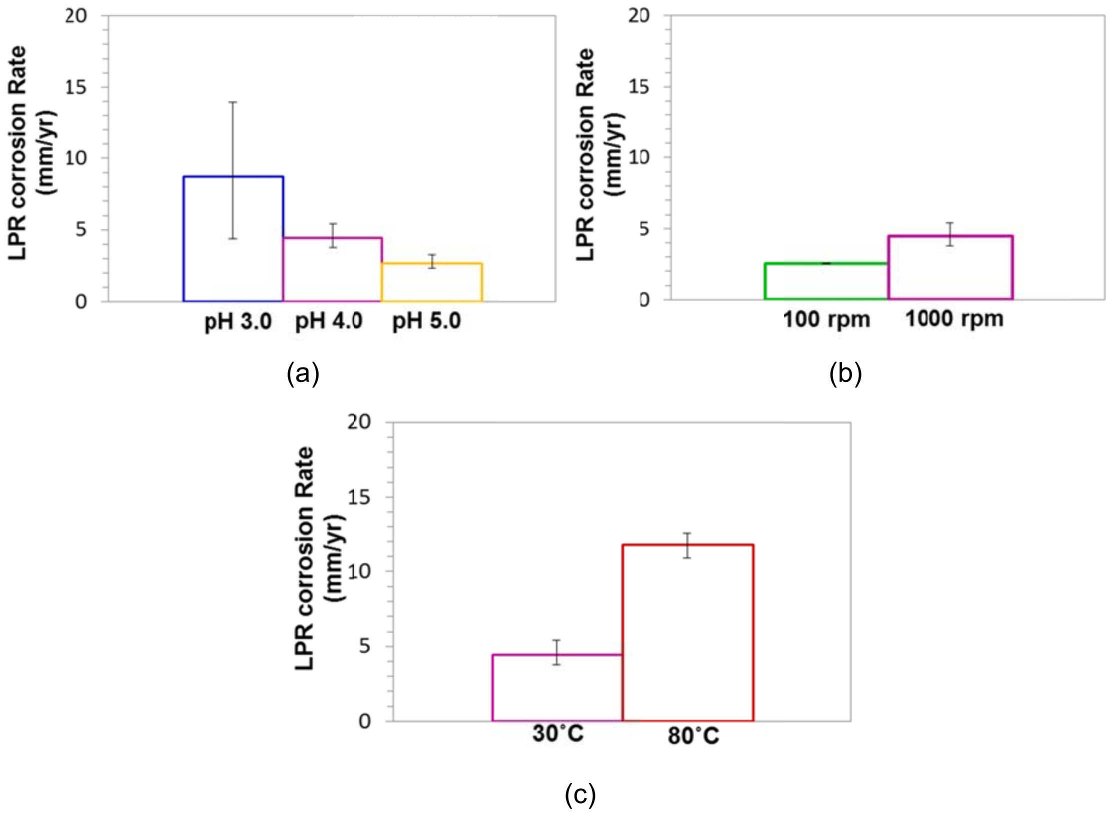

Figure 7. LPR uniform corrosion rate of API 5L X65 in a bulk solution (a) 0.096 MPa H_2S (960,000 ppm), 30˚C, 1000 rpm, (b) 0.96 bar H_2S, 30˚C, pH 4.0 , (C) 0.096 and 0.053 MPa H_2S, pH 4.0, 3 wt% NaCl, B= 23 mV/decade less than 2 hours exposure.

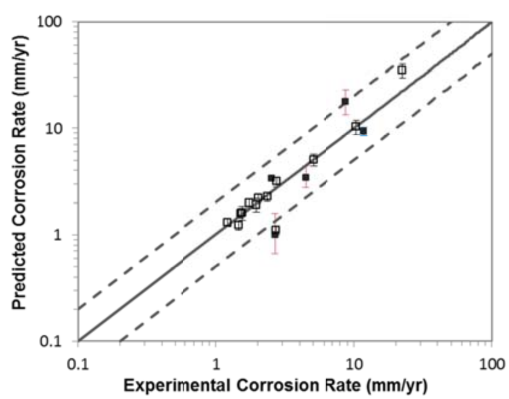

Figure 8. Parity plot of the predicted uniform corrosion rate using a mechanistic sour corrosion model [20] for short term exposure of mild steel to H_2S environments at different conditions in the absence of an iron sulfide layer on the surface *vs.* measured LPR corrosion rate.

CONCLUSIONS

- There is a lack of reliable, systematically collected, coherent corrosion data from experiments conducted at high pH_2S, based on sound electrochemical measurements. The present study was conducted to close this gap.
- It was found that the physico-chemical processes underlying H_2S corrosion in the absence of protective iron sulfides are very similar across a wide range of pH_2S.
- The existence of the so called "double wave" in the cathodic sweeps arises from the two independent cathodic reactions: H^+ reduction and direct H_2S reduction.
- It was demonstrated that the calculated corrosion rates based on the mechanistic corrosion model of Zheng, *et al.*, [20,25] are in reasonable agreement with the experimental data for a broad range of H_2S concentrations (up to 0.1 MPa partial pressure of H_2S).

ACKNOWLEDGMENT

The authors would like to thank the support of the following industrial sponsors: Anadarko, Baker Hughes, BP, Chevron, China National Offshore Oil Corporation, CNPC Tubular Goods Research Center, ConocoPhillips, DNV USA, ExxonMobil, M-I SWACO, Occidental Oil Company, Petroleum Institute, PTT, Saudi Aramco, Shell Global Solutions, SINOPEC, TOTAL, TransCanada, WGK.

REFERENCES

1. W. R. Whitney, "The Corrosion of Iron," Corrosion 3, (1947): p. 331-340.
2. D. C. Bond, and G. A. Marsh, "Corrosion of Wet Steel by Hydrogen Sulfide-Air Mixtures," Corrosion 6, 22 (1950): p. 22-28.
3. F. H. Meyer, O. L. Riggs, R. L. McGlasson, and J. D. Sudbury, "Corrosion Products of Mild Steel in Hydrogen Sulfide Environments," Corrosion 14, (1957): p. 69–75.
4. P. H. Tewari, and A. B. Campbell, "Dissolution of Iron during the Initial Corrosion of Carbon Steel in Aqueous H_2S Solutions" Can. J. Chem., 57, (1979): p. 188-196.
5. D. E. Milliams, C. J. Kroese, "Aqueous Corrosion of Steel by H2S and H_2S/CO_2 Mixture," Internal and External Protection of Pipes, (1979): p. 205–214.
6. J. B. Sardisco, and R. E. Pitts, "Corrosion of Iron in an H_2S-CO_2-H_2O System Composition and Protectiveness of the Sulfide Film as a Function of pH," Corrosion 21, (1965): p. 350–354.
7. J. B. Sardisco, and R. E. Pitts, "Corrosion of Iron in an H_2S-CO_2-H_2O System: Mechanism of Sulfide Film Formation and Kinetics of Corrosion Reaction," Corrosion 21, 245–253 (1965).
8. A. Dravnieks, and C. H. Samans, "Kinetics of Reaction of Steel with Hydrogen Sulfide-Hydrogen Mixtures," Electrochemical Society 105, (1958): p. 183-191.
9. E. C. Greco, and W. B. Wright, "Corrosion of Iron in an H_2S-CO_2-H_2O System. Corrosion 18, (1962): p. 119–124.
10. W. F. Rogers, and J. A. Rowe, "Corrosion Effect of Hydrogen Sulfide and Carbon Dioxide in Oil Production," in Fourth World Petroleum Congress (1955): p. 479-499.
11. S. N. Smith, and M. W. Joosten, "Corrosion of Carbon Steel by H_2S in CO_2 Containing Oilfield Environments," Corrosion/2005, paper no. 06115 (Houston, TX: NACE International, 2005).
12. P. W. Bolmer, "Polarization of Iron in H_2S-NaHS Buffers," National Association of Corrosion Engineering 21, (1965): p. 69–75.

13. B. Tribollet, J. Kittel, A. Meroufel, F. Ropital, F. Grosjean, E. M. M. Sutter, “Corrosion Mechanisms in Aqueous Solutions Containing Dissolved H_2S. Part 2 : Model of the Cathodic Reactions on a 316L Stainless Steel Rotating Disc Electrode,” Electrochimica Acta, 124, (2014): p.46–51.
14. S. P. Ewing, “Electrochemical Studies of the Hydrogen Sulfide Corrosion Mechanism,” Corrosion 11, (1955): p. 497–501.
15. J. B. Sardisco, W. B. Wright, and E. C. Greco, “Corrosion of Iron in an H_2S-CO_2-H_2O System: Corrosion Film Properties on Pure Iron,” Corrosion 19, (1963): p.354–359.
16. D. R. Morris, L. P. Sompaleanu, and D. N. Veysey, “The Corrosion of Steel by Aqueous Solutions of Hydrogen Sulfide,” J.Electrochem. Soc. 127, (1980): p.1228–1235.
17. A. Anderko, P. Mckenzie, R. D. Young, “Computation of Rates of General Corrosion Using Electrochemical and Thermodynamic Models,” Corrosion, 57 (2001): p. 202–213.
18. S. N. Smith, “A Proposed Mechanism for Corrosion in Slightly Sour Oil and Gas Production,” Corrosion/1993, paper no. 1304 (Houston, TX: NACE International, 1993).
19. W. Sun, and S. Nesic, “A Mechanistic Model of Uniform Hydrogen Sulfide/Carbon Dioxide Corrosion of Mild Steel,” Corrosion 65, (2009): p. 291–307.
20. Y. Zheng, B. Brown, and S. Nešic, “Electrochemical Study and Modeling of H_2S Corrosion of Mild Steel,” Corrosion 70 (2014): p. 351–365.
21. D. W. Shoesmith, P.Taylor, M. G. Bailey, and D. G. Owen, “The Formation of Ferrous Monosulfide Polymorphs during the Corrosion of Iron by Aqueous Hydrogen Sulfide at 21˚C,” J.Electrochem. Soc. 127, (1980): p. 1007–1015.
22. L. G. Benning, R. T. Wilkin, and H. Barnes, “Reaction Pathways in the Fe–S System below 100°C,” Chemical Geology 167, (2000): p. 25–51.
23. W. H. Thomason, “Formation Rates of Protective Iron Sulfide Films on Mild Steel in H_2S-Saturated Brine as a Function of Temperature,” Corrosion/1978, paper no. 41 (Houston, TX: NACE International, 1978).
24. I. H. Omar, Y. Gunaltun, J. Kvarekval, and A. Dugstad, “H_2S Corrosion of Carbon Steel under Simulated Kashagan Field Conditions,” Corrosion/2005, paper no. 05300 (Houston, TX: NACE International, 2005).
25. Y. Zheng, J. Ning, B. Brown, and S. Nešic, “Electrochemical Model of Mild Steel Corrosion in a Mixed H_2S/CO_2 Aqueous Environment in the Absence of Protective Corrosion Product Layers,” Corrosion 71, (2015): p. 316–325.
26. K. J. Lee, “A Mechanistic Modeling of CO_2 Corrosion of Mild Steel in the Presence of H2S,” (Ph.D diss., Ohio University, 2004).
27. J. Kvarekval, A. Dugstad, “Pitting Corrosion in CO_2/H_2S- Containing Glycol Solutions under Flowing Conditions,” Corrosion/2005, paper no. 05631 (Houston, TX: NACE International, 2005).
28. D. Abayarathna, “The Effect of Surface Films on Corrosion of Carbon Steel in a CO_2-H_2S-H_2O System,” Corrosion/2005, paper no. 05624 (Houston, TX: NACE International, 2005).
29. M. Liu, J. Wang, W. Ke, and E.-H. Han, “Corrosion Behavior of X52 Anti-H_2S Pipeline Steel Exposed to High H_2S Concentration Solutions at 90°C,” Journal of Materials Sci. Technol. 30, (2014): p. 504–510.
30. S. Navabzadeh Esmaeely, B. Brown, S. Nesic, “Verification of an Electrochemical Model for Aqueous Corrosion of Mild Steel for H_2S Partial Pressures up to 0.1 MPa”, Corrosion, (2016) . http://dx.doi.org/10.5006/2172.
31. A. Kahyarian, B. Bruce, and S. Nesic, “ Mechanism of Cathodic Reactions in Acetic Acid Corrosiobn of Iron and Mild Steel,” Corrosion, (2016) .http://dx.doi.org/10.5006/2177.